Economic Dispatch of Isolated Microgrids Based on Enhanced Sparrow Search Algorithm

Guodong Xie, Mengjian Zhang, Ming Yang, Deguang Wang

***Abstract*—To improve the economic efficiency and stability of microgrid operation, this study proposes an enhanced sparrow search algorithm (ESSA) for optimizing the economic dispatch (ED) in isolated microgrids. First, an elite opposition-based learning strategy is incorporated to mitigate the issue of premature convergence observed in SSA. Furthermore, an elite guidance mechanism and adaptive t disturbance are utilized to overcome the drawbacks of SSA, including low convergence accuracy and susceptibility to local optima. Finally, ESSA, along with five state-of-the-art swarm intelligence algorithms, is applied to address the microgrid economic dispatch problems in two representative climate scenarios. The experimental results demonstrate the superior performance of ESSA compared to the other five algorithms.**

***Index Terms*—isolated microgrid, economic dispatch, sparrow search algorithm, elite opposition-based learning, elite guidance mechanism, adaptive t disturbance.**

I. Introduction

THE issues of greenhouse effect and energy crisis have become critical global concerns [1], [2]. Within the realm of electric power, promoting the adoption of renewable energy sources is a viable strategy to address environmental challenges [3]. Among feasible solutions, microgrids, characterized by their compact size and diverse energy sources along with energy storage, have garnered interest owing to their flexibility and environmentally friendly power generation [4]. However, the increasing integration of renewable energy sources poses a significant challenge to the efficient management of microgrids due to the inherent uncertainty associated with these sources.

Economic dispatch (ED) [5] plays a crucial role in ensuring the stable and orderly operation of a microgrid. Within the constraints set by equipment capacity and system operations, the efficient operation and energy distribution of a microgrid can be accomplished through the careful allocation of power from distributed generation (DG) units and optimizing the dispatch of energy storage systems, contributing to the cost reduction in power supply.

Manuscript received November 21, 2023; revised February 12, 2024.

This work was supported in part by the National Natural Science Foundation of China under Grant 62341303, Grant 62203132 and Grant 52265066 and Guizhou Provincial Science and Technology Projects under Grant Qiankehejichu [ZK[2022]Yiban103].

Guodong Xie is a postgraduate student of the School of Electrical Engineering, Guizhou University, Guiyang 550025, China (e-mail: guod_xie@163.com)

Mengjian Zhang is a doctoral student of the School of Computer Science and Engineering, South China University of Technology, Guangzhou 510006, China (e-mail: 2311082906@qq.com)

Ming Yang is an associate professor of the School of Electrical Engineering, Guizhou University, Guiyang 550025, China (e-mail: myang23@gzu.edu.cn)

Deguang Wang is an associate professor of the School of Electrical Engineering, Guizhou University, Guiyang 550025, China (corresponding author to provide phone: 86-18292880795; e-mail: dgwang@gzu.edu.cn)

The optimal economic dispatch of microgrids is a multi-constrained and high-dimensional problem. Various approaches have been proposed to address the ED optimization problem of microgrids. Classical methods include quadratic programming [6], linear programming [7], and mixed-integer linear programming (MILP) [8]. Granelli et al. [9] solve the ED optimization problem based on sequential quadratic programming. Parisio et al. [10] employ MILP to reduce the ED cost of a microgrid. However, classical methods suffers from several limitations, including suboptimal performance and high computational resource requirements. Swarm intelligence (SI) algorithms, inspired by the cooperative behaviors of natural animal groups, have found widespread applications in addressing ED challenges in microgrids. Habib et al. [11] proposes a new honey beemating optimization algorithm to solve the ED problem. Basak et al. [12] combine crow search algorithm with JAYA to investigate the optimal dispatch of generator sets. Hassan et al. [13] utilize an enhanced beluga whale optimization algorithm to minimize the fuel cost. Dou et al. [14] consider demand response and apply particle swarm optimization (PSO) to reduce the economic dispatch cost of a microgrid. Raghav et al. [15] develope a framework based on quantum teaching learning optimization algorithm to increase the economic benefits in microgrid dispatch. Liu et al. [16] use quantum PSO to solve the economic objective function of a microgrid and reduce the economic cost.

Owing to the effectiveness in handling load fluctuations and the unpredictability of renewable energy sources, sparrow search algorithm (SSA) has been extensively employed to address various challenges in power systems. However, SSA suffers from slow convergence speed, easily trapping into local optima, and limited global search capability. In this study, an enhanced sparrow search algorithm (ESSA) is proposed for optimal economic dispatch of isolated microgrids.

1) Elite opposition-based learning, elite guidance mechanism, and adaptive t disturbance are incorporated into SSA, which enhance the performance of SSA in terms of the ability to jump from local optima, convergence speed, and convergence accuracy.
2) To evaluate the applicability and effectiveness of ESSA, two climate scenarios in the ED of microgrids are considered. The experimental results of ESSA and five comparison algorithms in two scenarios indicate the superiority of ESSA.

The remainder of this study is structured as follows. Section II provides the microgrid model and formulates the dispatch optimization problem for microgrids. Section III introduces SSA and proposes an enhanced SSA. Section IV presents an illustrative microgrid case study and compares the experimental results of the proposed ESSA with those of

five SI algorithms. Finally, Section V summarizes the main findings of this study and gives the potential directions for future research.

II. Problem formulation

In Fig. 1, the schematic diagram of an isolated microgrid is presented, where MT, PV, and WT are selected as DG units and SB acts as an energy storage unit.

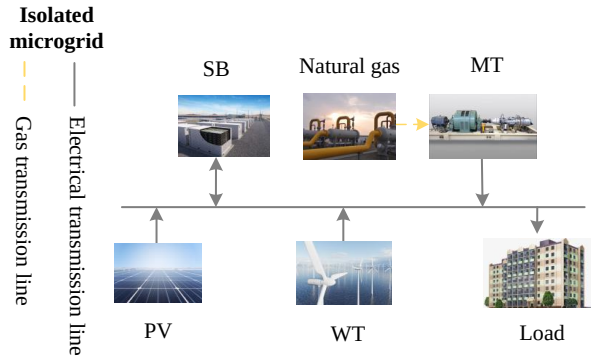

Fig. 1. Schematic diagram of an isolated microgrid.

A. Microgrid model

The output power of PV is calculated by:

$$P_{\mathrm{PV}}=\begin{cases} P_{\mathrm{PVr}}\cdot\dfrac{G_{\mathrm{c}}}{G_{\mathrm{STC}}}\cdot\left[1+k\cdot\left(T_{\mathrm{c}}-T_{\mathrm{r}}\right)\right], & G_{\mathrm{c}}>G_{\mathrm{tr}} \\ 0, & G_{\mathrm{c}}\le G_{\mathrm{tr}} \end{cases} \tag{1}$$

where P_{PVr} is the rated power; G_{c} is the illumination intensity; G_{tr} is the minimum illumination intensity; G_{STC} is the illumination intensity under standard test condition; T_{c} is the working temperature; T_{r} is the reference temperature.

The output power of WT is obtained by:

$$P_{\mathrm{WT}}=\begin{cases} 0, & 0\le v\le v_{\mathrm{ci}}\cup v\ge v_{\mathrm{co}} \\ P_{\mathrm{WTr}}\cdot\dfrac{v-v_{\mathrm{ci}}}{v_{\mathrm{r}}-v_{\mathrm{ci}}}, & v_{\mathrm{ci}}<v<v_{\mathrm{r}} \\ P_{\mathrm{WTr}}, & v_{\mathrm{r}}\le v\le v_{\mathrm{co}} \end{cases} \tag{2}$$

where P_{WTr} is the rated power; v_{ci} is the cut-in wind speed; v_{co} is the cut-out wind speed; v_{r} is the rated wind speed; v is the wind speed.

MT is a natural gas-fueled DG unit and its models are as follows:

$$Q_{\mathrm{MT}}=\frac{P_{\mathrm{MT}}\left(1-\eta_{\mathrm{MT}}-\eta_{l}\right)}{\eta_{\mathrm{MT}}} \tag{3}$$

$$Q_{\mathrm{ho}}=Q_{\mathrm{MT}}\times\eta_{\mathrm{rec}}\times COP_{\mathrm{ho}} \tag{4}$$

$$\eta_{rec}=\frac{T_0-T_2}{T_0-T_1} \tag{5}$$

where Q_{MT} represents the exhaust heat; P_{MT} is the output power of MT; η_{MT} is the unit efficiency of MT; η_l is the heat dissipation loss coefficient; Q_{ho} represents the generation capacity for waste heat of MT flue gas; COP_{ho} represents the heat coefficient; η_{rec} is the efficiency of waste heat recovery; T_0 and T_2 are the temperatures of flue gas entering and leaving the bromine cooler, respectively; T_1 is the environmental temperature.

The fuel cost of MT is calculated by:

$$C_{\mathrm{MTJ}}=C_{\mathrm{ng}}\times\frac{1}{LHV_{\mathrm{ng}}}\times\sum_{J}\frac{P_{\mathrm{MTJ}}}{\eta_{\mathrm{MTJ}}} \tag{6}$$

where C_{ng} is the price of natural gas; LHV_{ng} is the low calorific value of natural gas; P_{MTJ} is the output power of MT in a unit of time; η_{MTJ} is the efficiency in a unit of time.

As a buffer device, SB can improve the stability of the microgrid. The mathematical models of SB in the state of charge and discharge are described in Equations (7) and (8), respectively:

$$SOC_h=SOC_{h-1}\cdot(1-\sigma)+\eta_{\mathrm{c}}\cdot P_{\mathrm{ch}}^{h}\frac{\Delta h}{C_{\mathrm{r}}} \tag{7}$$

$$SOC_h=SOC_h\cdot(1-\sigma)+P_{\mathrm{dis}}^{h}\cdot\frac{\Delta h}{C_{\mathrm{r}}\cdot\eta_{\mathrm{d}}} \tag{8}$$

where σ is the discharging efficiency; η_{c} is the charging efficiency; $P_{\mathrm{ch}h}$ is the charging power at time h; C_{r} is the battery capacity; Δh is the unit of time; $P_{\mathrm{dis}h}$ is the discharging power; η_{d} is the discharging efficiency.

B. Dispatch model

(1) Objective function

The dispatch target of microgrid is to minimize the overall cost. The output of each DG unit is efficiently scheduled to meet the demand of load. Therefore, the objective function is:

$$\min\ C_{\mathrm{sum}}=C_1+C_2 \tag{9}$$

where C_1 is the operation cost; C_2 is the pollutant treatment cost.

The operation cost is expresses as:

$$C_1=\sum_{h=1}^{24}\left(K_{\mathrm{WT}}P_{\mathrm{WT}}^{h}+K_{\mathrm{PV}}P_{\mathrm{PV}}^{h}+K_{\mathrm{MT}}P_{\mathrm{MT}}^{h}+K_{\mathrm{bat}}\left(\left|P_{\mathrm{dis}}^{h}\right|+\left|P_{\mathrm{ch}}^{h}\right|\right)\right) \tag{10}$$

where K_{WT}, K_{PV}, and K_{MT} are the cost coefficients of WT, PV, and MT, respectively; K_{bat} represents the operation cost per hour of SB; P_{WT}^{h}, P_{PV}^{h}, and P_{MT}^{h} are the output powers of WT, PV, and MT at time h, respectively.

The pollutant treatment cost is expressed as:

$$C_2=\sum_{h=1}^{24}\left(\sum_{k=1}^{M}10^{-3}\cdot C_k\cdot r_k\cdot P_{\mathrm{MT}}^{h}\right) \tag{11}$$

where M is the number of pollutants; k is the type of pollutants; C_k and r_k are the external discounted cost and the emission coefficient of pollutant k, respectively.

(2) Constraints

To ensure the secure operation of the isolated microgrid, this study imposes constraints on SB, DG units, and load balance.

The constraints on SB are expressed as:

$$\begin{cases} P_{\mathrm{SB}}^{\min} \le P_{\mathrm{SB}} \le P_{\mathrm{SB}}^{\max} \\ P_{\mathrm{bat}}^{h} = P_{\mathrm{dis}}^{h} - P_{\mathrm{ch}}^{h} \\ 0 \le P_{\mathrm{dis}}^{h} \le P_{\mathrm{dis,max}}^{h} \times U_{\mathrm{dis}}^{h} \\ 0 \le P_{\mathrm{ch}}^{h} \le P_{\mathrm{ch,max}}^{h} \times U_{\mathrm{ch}}^{h} \\ U_{\mathrm{dis}}^{h} + U_{\mathrm{ch}}^{h} = 1 \\ \sum_{i=1}^{H} \left| U_{\mathrm{ch}}^{h} - U_{\mathrm{ch}}^{h-1} \right| \le N_{\mathrm{bat}} \end{cases} \tag{12}$$

where P_{SB} is the capacity of SB; $P_{\mathrm{SB}}^{\min}$ and $P_{\mathrm{SB}}^{\max}$ are the lower limit and upper limit of capacity of SB, respectively; P_{dis}^{h} and P_{ch}^{h} represent the discharging and charging powers of SB at time h; U_{dis}^{h} and U_{ch}^{h} are the state of SB at time h; $P_{\mathrm{dis,max}}^{h}$ and $P_{\mathrm{ch,max}}^{h}$ represent the maximum discharging power and maximum charging power of SB at time h; N_{bat} is the upper limit of SB in the states of charge and discharge; P_{bat}^{h} is the algebraic sum of charging and discharging powers of SB.

The ramp constraints on SB and MT are expressed as:

$$\begin{cases} -R_{\mathrm{MT}}^{\mathrm{down}} \cdot \Delta h \le P_{\mathrm{MT}}^{h} - P_{\mathrm{MT}}^{h-1} \le R_{\mathrm{MT}}^{\mathrm{up}} \cdot \Delta h \\ -R_{\mathrm{SB}}^{\mathrm{down}} \cdot \Delta h \le P_{\mathrm{SB}}^{h} - P_{\mathrm{SB}}^{h-1} \le R_{\mathrm{SB}}^{\mathrm{up}} \cdot \Delta h \end{cases} \tag{13}$$

where $R_{\mathrm{SB}}^{\mathrm{down}}$ and $R_{\mathrm{SB}}^{\mathrm{up}}$ represent the downward and upward ramp rates of SB, respectively; $R_{\mathrm{MT}}^{\mathrm{down}}$ and $R_{\mathrm{MT}}^{\mathrm{up}}$ represent the downward and upward ramp rates of MT, respectively.

The constraints on load can be expressed as:

$$P_{\mathrm{SB}}^{h} + P_{\mathrm{MT}}^{h} + P_{\mathrm{WT}}^{h} + P_{\mathrm{PV}}^{h} = P_{\mathrm{L}}^{h} \tag{14}$$

where P_{SB}^{h}, P_{MT}^{h}, P_{WT}^{h}, and P_{PV}^{h} denote the output powers of SB, MT, WT, and PV at time h, respectively; P_{L}^{h} denotes the electric load power.

III. Methodology

A. Sparrow search algorithm

In SSA, the population is categorized into three groups: producers, scroungers, and danger perceivers [18]. Let n represent the population size. The locations of sparrows are put in the matrix:

$$Y = \begin{bmatrix} y_{1,1} & \cdots & y_{1,d} \\ \vdots & & \vdots \\ y_{n,1} & \cdots & y_{n,d} \end{bmatrix} \tag{15}$$

where d is the dimension of design variables.

The fitness values of the population are stored in the vector:

$$F_Y = \begin{bmatrix} f\left(\begin{bmatrix} y_{1,1} & \cdots & \cdots & y_{1,d} \end{bmatrix}\right) \\ f\left(\begin{bmatrix} y_{2,1} & \cdots & \cdots & y_{2,d} \end{bmatrix}\right) \\ \vdots \\ f\left(\begin{bmatrix} y_{n,1} & \cdots & \cdots & y_{n,d} \end{bmatrix}\right) \end{bmatrix} \tag{16}$$

where f is the fitness function.

The formula for the position update of producers is:

$$Y_{i,j}^{T+1} = \begin{cases} Y_{i,j}^{T} \cdot \exp\left(\dfrac{-i}{\alpha \cdot T_{\max}}\right), & R_2 < ST \\ Y_{i,j}^{T} + Q \cdot M_L, & R_2 \ge ST \end{cases} \tag{17}$$

where T is the iteration number; $y_{i,j}^{T}$ indicates the location of the ith individual in the j dimensional space; $\alpha \in (0, 1]$ is a random number; $T_{\max}$ represents the maximum iteration number; Q is a random number that follows a normal distribution; M_L is a matrix of $1 \times d$ with each of its elements being 1; $R_2 \in [0, 1]$ and $ST \in [0.5, 1.0]$ denote the alarm and safety values, respectively.

Scroungers adjust their locations by tracking the most well-adapted producers. The location update formula of scroungers is expressed as:

$$Y_{i,j}^{T+1} = \begin{cases} Q \cdot \exp\left(\dfrac{Y_{\mathrm{worst}}^{T} - Y_{i,j}^{T}}{i^2}\right), & i > n/2 \\ Y_{\mathrm{P}}^{T+1} + \left| Y_{i,j}^{T} - Y_{\mathrm{P}}^{T+1} \right| \cdot A^{+} \cdot M_L, & i \le n/2 \end{cases} \tag{18}$$

where Y_{P}^{T+1} represents the optimal location; Y_{worst}^{T} represent the worst location in the current space; A represents a $1 \times d$ matrix with the element values randomly chosen as 1 or -1.

Danger perceivers are randomly distributed within the population, comprising approximately 10% to 20%. Their locations are updated according to:

$$Y_{i,j}^{T+1} = \begin{cases} Y_{\mathrm{best}}^{T} + \beta \cdot \left| Y_{i,j}^{T} - Y_{\mathrm{best}}^{T} \right|, & f_i > f_{\mathrm{g}} \\ Y_{i,j}^{T} + K \cdot \left(\dfrac{\left| Y_{i,j}^{T} - Y_{\mathrm{worst}}^{T} \right|}{(f_i - f_{\mathrm{w}}) + \varepsilon} \right), & f_i = f_{\mathrm{g}} \end{cases} \tag{19}$$

where β represents a random number that follows a normal distribution; Y_{best}^{T} represents the best global location during the tth iteration; $K \in [-1, 1]$ is a random number, f_i represent the current fitness values, f_{w}, and f_{g} are the current optimal and worst fitness values, respectively; ε is a small constant used to prevent division by zero errors.

B. Enhanced sparrow search algorithm

(1) Initialization strategy

SSA employs a pseudo-random approach to initialize the population, which can potentially result in premature convergence. In response to the issue, this study incorporates the elite opposition-based learning strategy [19]:

$$\overline{Y}_{i,j}^{\mathrm{E}} = \tau \cdot (L_j + U_j) - Y_{i,j} \tag{20}$$

where $\overline{Y}_{i,j}^{\mathrm{E}}$ is the elite opposite solution; U_j and L_j represent the upper and lower bounds, respectively; τ is a random number in the interval [0,1]; $Y_{i,j} \in [L_j, U_j]$ is the current solution. If $\overline{Y}_{i,j}^{\mathrm{E}}$ exceeds the bounds, then it is replaced by:

$$\overline{Y}_{i,j}^{\mathrm{E}} = \mathrm{rand}\left(\mathrm{L_j} + \mathrm{U_j}\right) \tag{21}$$

(2) Elite guidance mechanism

To overcome the disadvantage of slow convergence that SSA faces, this study utilizes an elite guidance mechanism [20] to update the locations of producers.

$$Y_{i,j}^{T+1} = \begin{cases} Y_{i,j}^{T} \cdot \exp\left(\dfrac{-i}{\alpha \cdot T_{\max}}\right), & R_2 < ST\& \\ & R_3 > p_{co} \\ Y_{i,j}^{T} + Q \cdot L, & R_2 \ge ST\& \\ & R_3 > p_{co} \\ Y_{\mathrm{best}}^{T} \cdot \exp\left(\dfrac{-i}{\alpha \cdot T_{\max}}\right), & R_2 < ST\& \\ & R_3 \le p_{co} \\ Y_{\mathrm{best}}^{T} + Q \cdot L, & R_2 \ge ST\& \\ & R_3 \le p_{co} \end{cases} \tag{22}$$

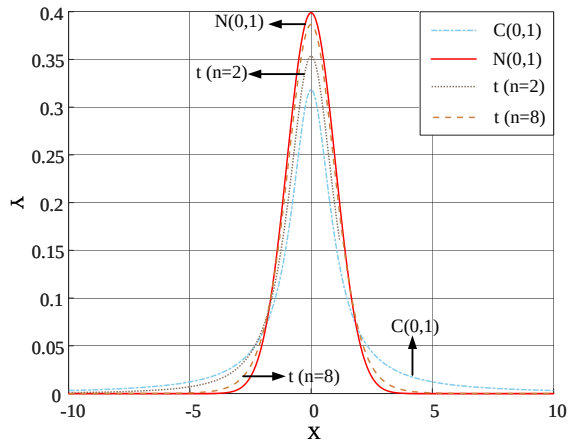

Fig. 2. Probability density diagrams of three distributions.

where $R_3 \in [0,1]$ is a random number; p_{co} is the control parameter, which is expressed as:

$$p_{co} = 0.4 - 0.4 \cdot \frac{T}{T_{\max}} \tag{23}$$

The parameter p_{co} is used to regulate the transformation of the position update of producers. In the early phase of iteration, where there are fewer elite individuals in the population and p_{co} has a higher value, producers are more inclined to utilize the last two terms of Equation (22) for location update. As the iteration continues and the value of p_{co} decreases, the influence of the elite guidance mechanism diminishes and producers tend to revert to the original update mode.

(3) Adaptive t disturbance

SSA tends to converge towards the optimal individual in later iterations, which results in the reduced population diversity and a susceptibility to local optima. To overcome these drawbacks, an adaptive t disturbance [21] is employed in this study.

In Fig. 2, probability density diagrams are provided for Gaussian, Cauchy, and t distributions at various degrees of freedom. It is obvious that Gaussian distribution has a limited disruptive effect and struggles to guide the algorithm away from local optima. In contrast to Gaussian distribution, Cauchy distribution exhibits superior characteristics with a two-wing distribution, leading to a wider range. However, in the later stage of iterations, as the population converges towards the global optima, smaller disturbances become essential to enhance the local search capability of the algorithm. Consequently, an adaptive t disturbance with adjustable parameters can address the limitations of both Gaussian and Cauchy disturbances. The expression of the adaptive t disturbance is described as:

$$Y_{i,j}^{T+1} = Y_{i,j}^{T} + t(R_T) \cdot Y_{i,j}^{T} \tag{24}$$

where $t(R_T)$ is a random number obeying t distribution. The calculation formula of R_T is:

$$R_T = \mathrm{INT}\left(30 \cdot \frac{T}{T_{\max}}\right) \tag{25}$$

The flowchart of ESSA is presented in Fig. 3. The primary steps are outlined as follows:

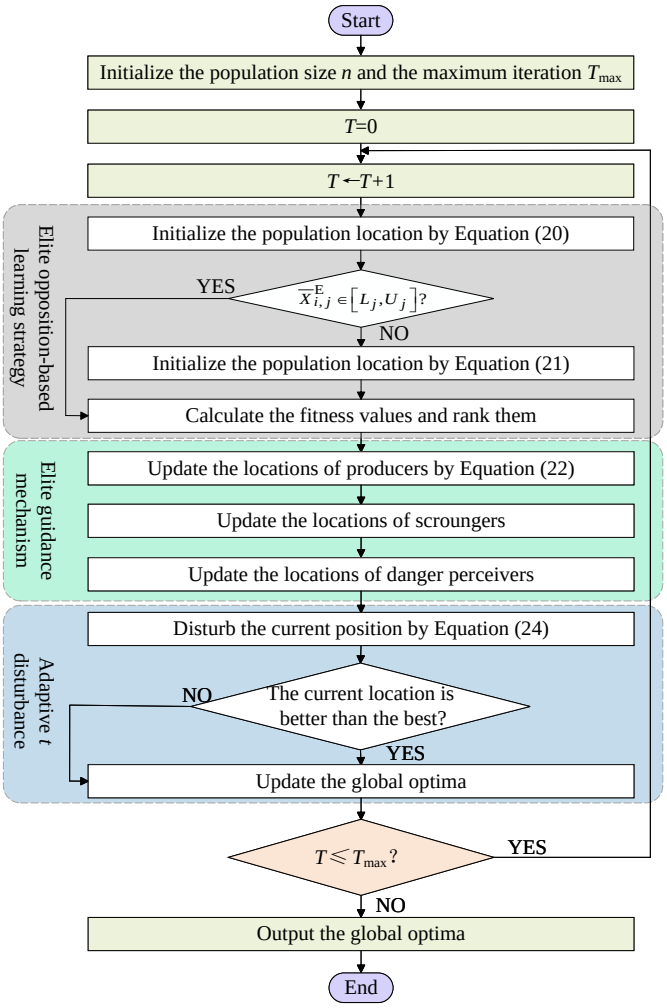

Fig. 3. Flowchart of ESSA

1) Set the parameters, including the dimension of design variables, population size, and maximum iteration number.
2) Initialize the population position by Equation (20).
3) Use Equation (22) to update the positions of producers for facilitating the acceleration of convergence speed.
4) Use Equation (24) to perturb the population position for escaping from local optima and enhancing convergence accuracy.
5) Output the global optima once the maximum iteration number is reached.

IV. Experimental Results and Analysis

To evaluate the effectiveness and superiority of ESSA, two typical climate scenarios are considered. All experiments are carried out using MATLAB 2022a on a Windows 11 platform, utilizing a computer equipped with 256 GB of RAM and an AMD R7-5800H CPU. Each algorithm is independently executed 30 times, with the maximum iteration number set to 500.

A. Parameter setting and scenario description

The isolated microgrid in the experiment consists of PV, WT, SB, and MT. Detailed module parameters are provided in Table I.

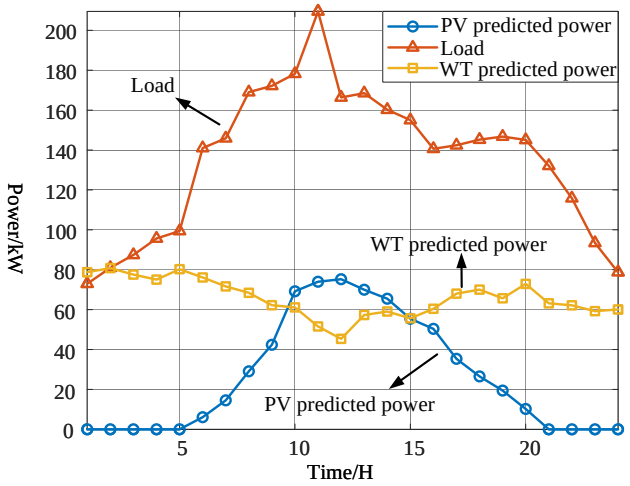

(a) Power prediction curves of PV, WT, and load in Scenario 1

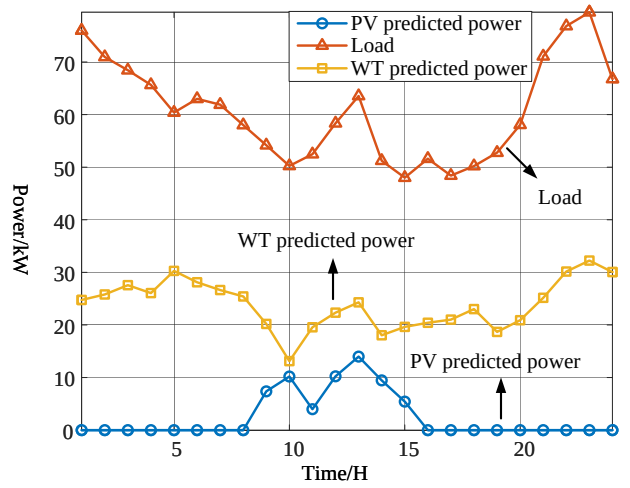

(b) Power prediction curves of PV, WT, and load in Scenario 2

Fig. 4. Power prediction curves of PV, WT, and load.

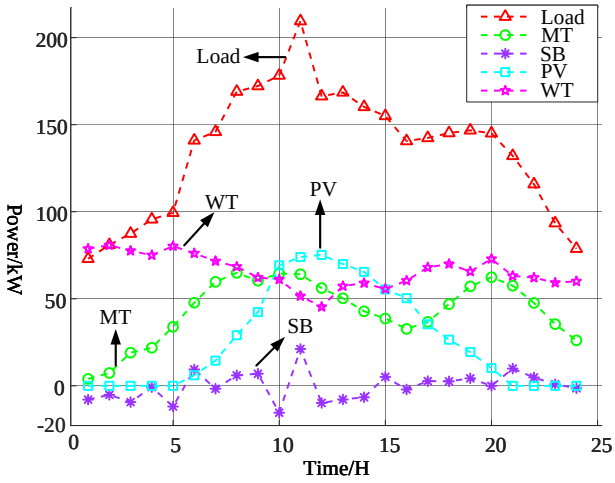

(a) The output power of each DG unit in Scenario 1

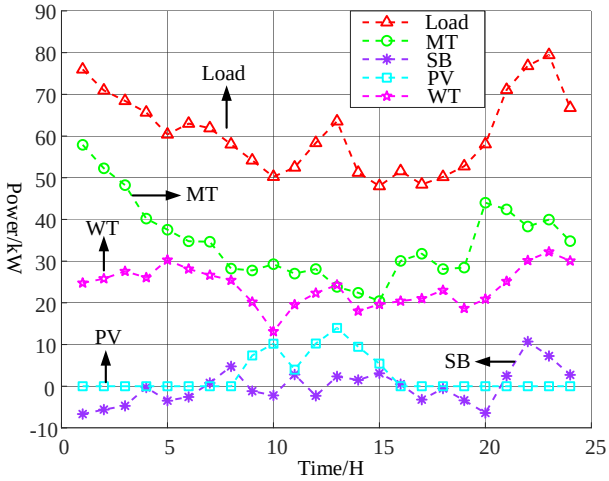

(b) The output power of each DG unit in Scenario 2

Fig. 5. The output power of each DG unit obtained by ESSA.

TABLE I
TECHNICAL PARAMETERS OF WT, PV, MT, AND SB.

	WT	PV	MT	SB
Upper limit of output (kW)	80	40	65	40
Lower limit of output (kW)	0	0	0	−40
Maintenance coefficient (yuan/kW)	0.298	0.010	0.031	0.001

Two typical climate scenarios are described as follows:

Scenario 1: The presence of abundant natural resources results in significant power generation from both MT and PV.

Scenario 2: The scarcity of natural resources leads to restricted power generation from both MT and PV.

The isolated microgrid operates on a 24-hour dispatch cycle, with each hour considered as the fundamental time period. The Power prediction curves of PV, WT, and load in Scenarios 1 and 2 are depicted in Figs. 4(a) and 4(b), respectively.

The parameter settings of ESSA, sparrow search algorithm (SSA), particle swarm optimization (PSO) [22], harris hawks optimization (HHO) [23], artificial ecosystem-based optimization (AEO) [24], and zebra optimization algorithm (ZOA) [25] are presented in Table II.

B. Scenario 1

The output power of each DG unit in Scenario 1 obtained by ESSA is presented in Fig. 5(a). It is observed that MT and WT primarily function as output units from 23:00 to 5:00. During the period of increased load from 6:00 to 23:00, WT, PV, SB, and MT collaborate to keep the stability of the microgrid. SB serves as a buffer device, transitioning between charging and discharging states at different time intervals and operational modes.

Table III lists the dispatch results of ESSA and five state-of-the-art algorithms. ESSA achieves the lowest average generation cost in Scenario 1, even though its performance is not optimal in terms of variance. Specifically, the average generation cost of ESSA is 1498.3. In comparison to SSA, PSO, HHO, AEO, and ZOA, the average generation cost of ESSA is reduced by 0.11%, 0.16%, 0.95%, 0.22%, and 0.54%, respectively.

The box plot is a data visualization tool that illustrates the degree of data dispersion and the stability of optimization results. To further visualize the distribution of dispatch results of six algorithms, the box plot representing the generation costs of dispatch results in Scenario 1 is presented in Fig. 6(a). The median of the box plot of ESSA is 1498.6, while the medians of the box plots of the other five algorithms

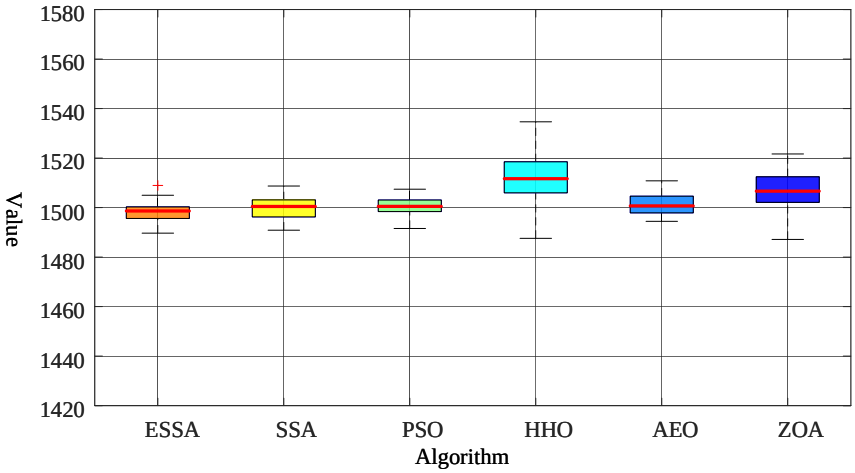

(a) Box plot of six algorithms in Scenario 1

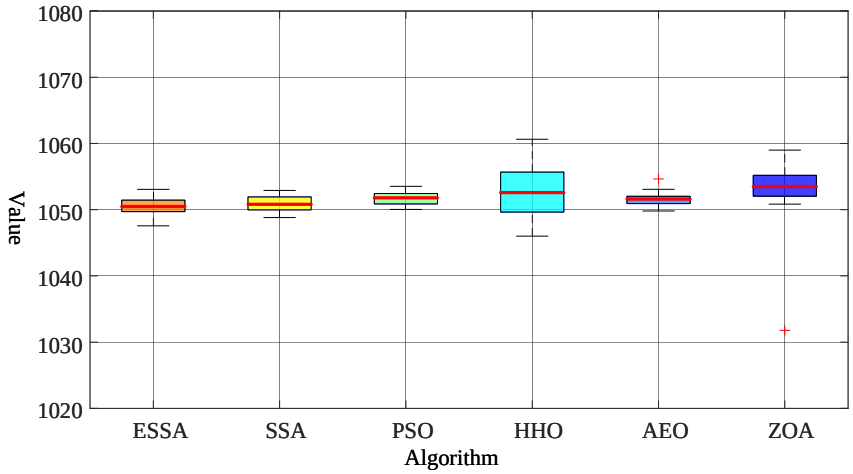

(b) Box plot of six algorithms in Scenario 2

Fig. 6. Box plots of six algorithms.

TABLE II
PARAMETER SETTINGS OF ESSA AND FIVE COMPARISON ALGORITHMS.

Algorithm	Parameter
ESSA	N=50, ST=0.8, PD=0.2, SD=0.1 , $P = 0.4 - 0.4(T/T_{\max})$
SSA	N=50, ST=0.8, PD=0.2, SD=0.1
PSO	N=50, $c1$=1.5, $c2$=2.0, w=1
HHO	N=50
AEO	N=50, $r1$,$r2$,$r3 \in [-1, 1]$
ZOA	N=50

are 1500.4, 1500.5, 1511.6, 1500.6, and 1506.6, respectively. Consequently, the box plot of ESSA is at the lowest level, indicating that the overall quality of solutions obtained by ESSA is superior to that of the other five algorithms. Furthermore, the interquartile range (IQR) of the box plot of ESSA is 4.69, while the IQRs of the other five algorithms are 6.86, 4.65, 12.52, 6.73, and 10.3, respectively. To sum up, ESSA exhibits superior data distribution compared with the other five algorithms.

C. Scenario 2

The output power of each DG unit in Scenario 2 obtained by ESSA is presented in Fig. 5(b). Although Scenario 2 experiences a lower user load than Scenario 1, the output ratio of MT in Scenario 2 significantly rises, attributed to the scarcity of natural resources. As a result, MT serves as the primary output unit to ensure the stable operation of the microgrid.

The dispatch results of ESSA and five SI algorithms in Scenario 2 are provided in Table III. Although the dispersion of dispatch results of ESSA is higher than that of SSA, PSO, and AEO, the average generation cost of ESSA is 1050.5. In comparison to SSA, PSO, HHO, AEO, and ZOA, the average generation cost of ESSA is reduced by 0.03%, 0.12%, 0.03%, 0.10%, and 0.22%, respectively. The box plot of dispatch results is displayed in Fig. 6(b). As seen, the medians of the box plots of ESSA, SSA, PSO, HHO, AEO, and ZOA are 1050.4, 1050.8, 1051.8, 1052.6, 1051.6, and 1053.5, respectively. In addition, the IQRs of the box plots of ESSA, SSA, PSO, HHO, AEO, and ZOA amount to 1.7, 1.9, 1.5, 6.0, 1.1, and 3.1, respectively.

TABLE III
OPTIMIZATION RESULTS OBTAINED BY ESSA AND FIVE COMPARISON ALGORITHMS IN SCENARIOS 1 AND 2.

Scenario	Metric	ESSA	SSA	PSO	HHO	AEO	ZOA
Scenario 1	Avg (Yuan)	**1498.3**	1500.0	1500.7	1512.6	1501.6	1506.4
	Worst (Yuan)	1509.0	1508.7	**1507.4**	1534.7	1510.8	1521.7
	Best (Yuan)	1489.7	1490.9	1491.6	1487.6	1494.4	**1487.1**
	Std	3.9	4.6	**3.7**	10.3	4.4	8.6
Scenario 2	Avg (Yuan)	**1050.5**	1050.8	1051.8	1050.8	1051.6	1053.1
	Worst (Yuan)	1053.1	**1052.9**	1053.5	1060.6	1054.6	1059.0
	Best (Yuan)	1047.6	1048.8	1050.0	1046.0	1049.8	**1031.8**
	Std	1.4	1.2	**0.9**	4.0	1.0	4.5

According to the earlier experimental results and analysis, the comprehensive evaluation of dispatch results in Table III and the positions in the box plots reveal that ESSA holds a clear advantage despite SSA, PSO, and AEO showing superiority in specific metrics. In two typical climate scenarios, the box plots of ESSA consistently locate at the lower positions, with its average generation cost being lower than the other five SI algorithms. This indicates the superior capacity of ESSA in addressing the economic dispatch optimization problem in microgrids, effectively avoiding local optima to identify enhanced dispatch solutions.

V. CONCLUSION AND FUTURE WORK

Due to the randomness and volatility of renewable energy sources, the economic dispatch optimization problem of isolated microgrids is a challenging task. In order to efficiently solve this problem, this study proposes an enhanced sparrow search algorithm (ESSA). Three improved strategies, namely, elite opposition-based learning, elite guidance mechanism, and adaptive t disturbance, are integrated into SSA, which overcome the drawbacks of slow convergence speed, susceptibility to local optima, and limited global search capability. To demonstrate the effectiveness and applicability of ESSA, two typical climate scenarios in the economic dispatch of microgrids are taken into account. The experimental results of ESSA are compared with those of five state-of-the-art optimization algorithms. In terms of energy utilization and generation cost, ESSA outperforms the other five algorithms in two scenarios.

This study solely addresses the single-objective dispatch of microgrids. Future work will focus on the optimization problem involving both economic and environmental aspects in microgrid dispatch.

REFERENCES

[1] J. Li, S. Sun, D. Sharma, et al, "Tracking the drivers of global greenhouse gas emissions with spillover effects in the post-financial crisis era," *Energy Policy*, vol. 174, pp. 113464, 2023.

[2] M. B. Niu, H. C. Wang, J. Li, et al, "Coordinated energy dispatch of highway microgrids with mobile storage system based on DMPC optimization," *Electric Power Systems Research*, vol. 217, pp. 109119, 2023.

[3] W. G. Zhang, Q. Zhu, H. J. Zheng, et al, "Economic and optimal dispatch model of electricity, heat and gas for virtual power plants in parks considering low carbon targets," *Engineering Letters*, vol. 31, no. 1, pp. 93–104, 2023.

[4] A. Cagnano, E. D. Tuglie, P. Mancarella, "Microgrids: Overview and guidelines for practical implementations and operation," *Applied Energy*, vol. 258, pp. 114039, 2020.

[5] X. Wang, R. P. Liu, X. Wang, et al, "A data-driven uncertainty quantification method for stochastic economic dispatch," *IEEE Transactions on Power Systems*, vol. 37, no. 1, pp. 812–815, 2021.

[6] N. Nabona, L. L. Freris, "Optimisation of economic dispatch through quadratic and linear programming," In Proceedings of the Institution of Electrical Engineers, vol. 120, no. 5, pp. 574–580, 1973.

[7] A. A. El-Keib, H. Ding, "Environmentally constrained economic dispatch using linear programming," *Electric Power Systems Research*, vol. 29, no. 3, pp. 155–159, 1994.

[8] C. L. Chen, "Non-convex economic dispatch: a direct search approach," *Energy Conversion and Management*, vol. 48, no. 1, pp. 219–225, 2007.

[9] G. P. Granelli, M. Montagna, "Security-constrained economic dispatch using dual quadratic programming," *Electric Power Systems Research*, vol. 56, no. 1, pp. 71–80, 2000.

[10] A. Parisio, L. Glielmo, "A mixed integer linear formulation for microgrid economic scheduling," In Proceedings of IEEE International Conference on Smart Grid Communications, pp. 505–510, 2011.

[11] S. Habib, M. A. Kamarposhti, H. Shokouhandeh, et al, "Economic dispatch optimization considering operation cost and environmental constraints using the HBMO method," *Energy Reports*, vol. 10, pp. 1718–1725, 2023.

[12] S. Basak, B. Bhattacharyya, B. Dey B, "Dynamic economic dispatch using hybrid CSAJAYA algorithm considering ramp rates and diverse wind profiles," *Intelligent Systems with Applications*, vol. 16, pp. 200116, 2022.

[13] M. K. Hassan, S. Kamel, F. Jurado, et al, "Economic load dispatch solution of large-scale power systems using an enhanced beluga whale optimizer," *Alexandria Engineering Journal*, vol. 73, pp. 573–591, 2023.

[14] C. Dou, X. Zhou, T. Zhang, et al, "Economic optimization dispatching strategy of microgrid for promoting photoelectric consumption considering cogeneration and demand response," *Journal of Modern Power Systems and Clean Energy*, vol. 8, no. 3, pp. 557–563, 2020.

[15] L. P. Raghav, R. S. Kumar, D. K. Raju, et al, "Optimal energy management of microgrids using quantum teaching learning based algorithm," *IEEE Transactions on Smart Grid*, vol. 12, no. 6, pp. 4834–4842 2021.

[16] X. M. Liu, M. Zhao, Z. H. Wei, et al, "The energy management and economic optimization scheduling of microgrid based on colored petri net and quantum-PSO algorithm," *Sustainable Energy Technologies and Assessments*, vol. 53, pp. 102670, 2022.

[17] H. Long, Z. Chen, H. Huang, et al, "Research on multi-objective optimization power flow of power system based on improved remora optimization algorithm," *Engineering Letters*, vol. 31, no. 3, pp. 1191–1207, 2023.

[18] J. Xue , B. Shen, "A novel swarm intelligence optimization approach: sparrow search algorithm," *Systems Science & Control Engineering*, vol. 8, no. 1, pp. 22–34, 2020.

[19] X. Zhou, Z. Wu, H. Wang, "Elite opposition-based differential evolution for solving large-scale optimization problems and its implementation on GPU," In Proceedings of the 13th International Conference on Parallel and Distributed Computing, Applications and Technologies, pp. 727–732, 2012.

[20] Y. Li, S. Wang, B. Yang, "An improved differential evolution algorithm with dual mutation strategies collaboration," *Expert Systems with Applications*, vol. 153, pp. 113451, 2020.

[21] H. Zhang, Q. Huang, L. Ma, et al, "Sparrow search algorithm with adaptive t distribution for multi-objective low-carbon multimodal transportation planning problem with fuzzy demand and fuzzy time," *Expert Systems with Applications*, vol. 238, pp. 122042, 2024.

[22] J. Kennedy, R. Eberhart, "Particle swarm optimization," In Proceedings of the 1995 IEEE International Conference on Neural Networks, vol. 4, pp. 1942–1948, 1995.

[23] A. A. Heidari, S. Mirjalili, H. Faris, et al, "Harris hawks optimization: Algorithm and applications," *Future Generation Computer Systems*, vol. 97, pp. 849–872, 2019.

[24] W. Zhao, L. Wang, Z. Zhang, "Artificial ecosystem-based optimization: a novel nature-inspired meta-heuristic algorithm," *Neural Computing and Applications*, vol. 32, pp. 9383–9425, 2020.
[25] E. Trojovska, M. Dehghani, P. Trojovsky, "Zebra optimization algorithm: A new bio-inspired optimization algorithm for solving optimization algorithm," *IEEE Access*, vol. 10, pp. 49445–49473, 2022.